BAMS Map Room

# Pacific–North American Teleconnection Tumbles Snowfall Records West of the Cascades during Christmas Week 2021

Bin Guan and Sumant Nigam

**ABSTRACT:** During the week of Christmas 2021, winter storms pummeled the Pacific Northwest and broke daily temperature and snowfall records in scores, especially west of the Cascades and notably in Oregon. With La Niña ruling the tropical Pacific, the record-setting, disruptive snowfall during Christmas week raised questions about its origin, especially as the seasonal outlook was for below-normal precipitation. We show that Pacific–North American (PNA) teleconnection—a well-documented subseasonal variability pattern during winter—reigned over the region in its negative phase; it was the strongest 7-day PNA episode in December in more than 50 years. It led to robust northwesterly onshore flow, whose interaction with the Coastal, Cascade, and Sierra ranges led to blockbuster snowfall and precipitation. Note that one seldom encounters circulation anomalies consisting of just one winter teleconnection pattern. Also worth noting is the tremendous power of *subseasonal* variability in recharging Western water resources in the context of the *seasonal* gloom from a La Niña–intensified West Coast drought.

**KEYWORDS:** Teleconnections; Drought; Extreme events; La Nina; Snowfall; Subseasonal variability

https://doi.org/10.1175/BAMS-D-22-0021.1

Corresponding author: Sumant Nigam, nigam@umd.edu

In final form 13 June 2023

**AFFILIATIONS: Guan**—Joint Institute for Regional Earth System Science and Engineering, University of California, Los Angeles, Los Angeles, and Jet Propulsion Laboratory, California Institute of Technology, Pasadena, California; **Nigam**—Department of Atmospheric and Oceanic Science, University of Maryland, College Park, College Park, Maryland

The week of Christmas 2021 brought unsettled weather to the Pacific Northwest, with strong storms battering the region and heavy snow and cold temperatures snarling holiday travel. Daily temperature and snowfall records were broken in scores, especially west of the Cascades and notably in Oregon; precipitation records were also set in the Sierra Nevada. With La Niña ruling the tropical Pacific, seasonal precipitation along the U.S. West Coast was predicted to be below normal. While that does not forbid above-normal precipitation in any particular week, the record-setting, disruptive snowfall during Christmas week raised questions about its origin. Was it a confluence of winter teleconnection patterns or a single amplified pattern?

Of interest is the Pacific–North American (PNA) teleconnection, which has been shown to be closely linked to hydroclimatic variability and extremes in the western United States in previous studies. For example, Cayan (1996) showed that anomalously low seasonal snowpack in most of the western United States was associated with winter circulation that resembles the positive phase of PNA. With a high-pressure anomaly over the Pacific Northwest in the positive phase, the PNA pattern directs storms northward and away from the region, leading to prolonged precipitation deficits in this phase. Ge and Gong (2009) showed the North American average December snow depth to be most strongly (and negatively) correlated with the PNA, with correlations strongest in the western United States. Guan et al. (2013) found that wintertime atmospheric rivers—major precipitation deliverers, flood producers, and drought busters in the western United States (e.g., Ralph et al. 2006; Guan et al. 2010; Dettinger 2013)—make landfall in California 50% more frequently during PNA's negative phase. The result is consistent with the comprehensive analysis of Guan and Waliser (2015), which showed PNA to be the strongest modulator of winter atmospheric river frequency in the western United States from comparing the influence of various large-scale teleconnection patterns.

In this study, we focus on the role of PNA in generating record-setting snowstorms during the Christmas week of 2021. An examination of specific PNA episodes and their hydroclimate impacts on submonthly time scales remains lacking despite the progress in understanding PNA's seasonal footprints. Analyzing the 2021 Christmas week's circulation and snowfall provides an opportunity to fill this gap. We highlight the weekly large-scale and regional conditions that contributed to the setting of daily snowfall records in the Pacific Northwest.

## An exceptionally strong negative PNA

The PNA is one of the leading modes of subseasonal climate variability in Northern Hemisphere winter. It is characterized by a coherent arcing pattern of height fluctuations of alternating signs, beginning with a center over Hawaii and followed by centers over the tip of the Aleutians, northwestern North America, and southeastern United States (shown in Fig. 1c by its 300-hPa signature). In the positive phase (depicted), the pattern consists of

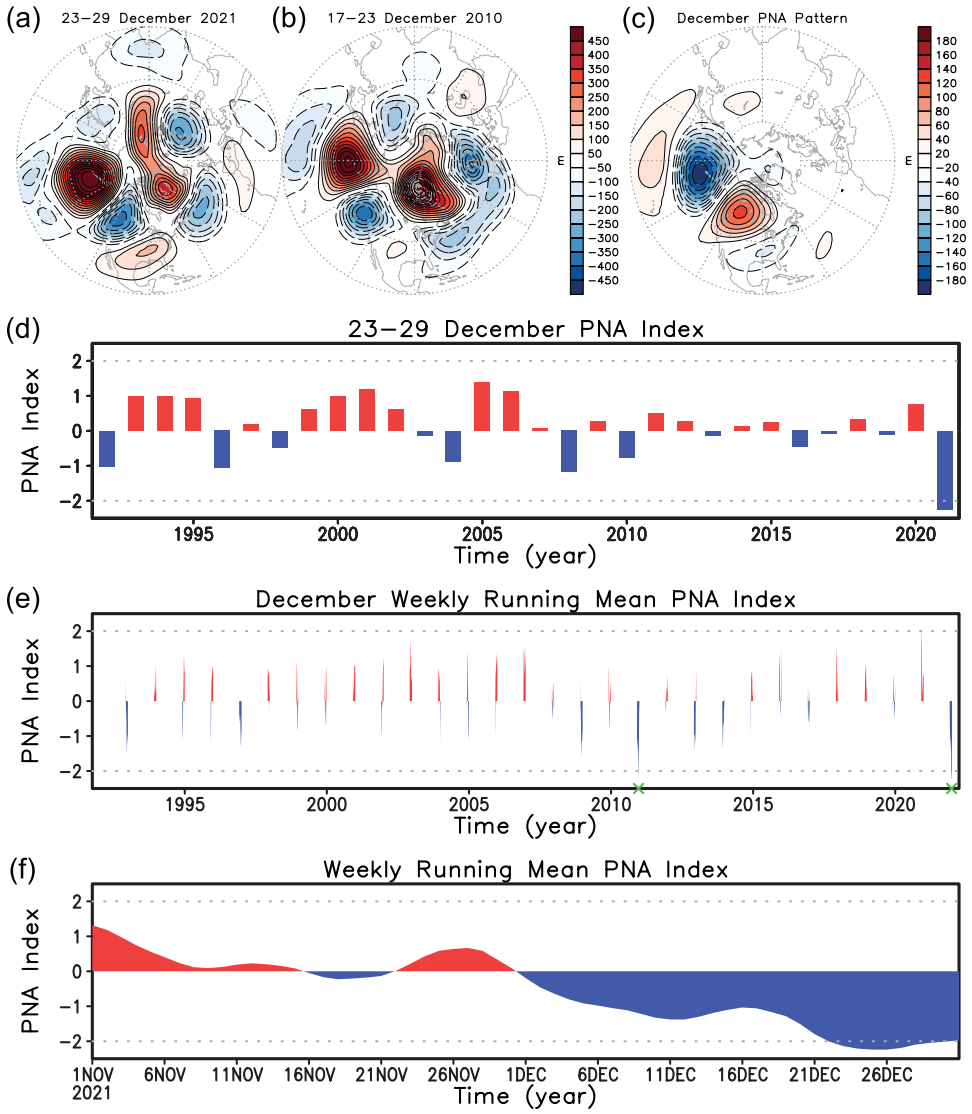


**Fig. 1. (a) Mean 300-hPa geopotential height anomalies (m) during 23–29 Dec 2021. Anomalies are relative to the 1992–2021 climatology. The same 30-yr period is used in all subsequent figures. (b) As in (a), but for 17–23 Dec 2010. (c) The canonical positive-phase pattern of PNA in December, based on regressing 300-hPa geopotential height anomalies to the December PNA index. (d) Seven-day mean PNA index during 23–29 Dec each year. (e) Seven-day running means based on the daily PNA index; only December values are shown. The two green × symbols mark the top two negative PNA episodes analyzed in this study. (f) The weekly running-mean PNA index during November–December 2021. The dotted lines in (d)–(f) indicate ±2 standard deviations of the year-round daily PNA index. Geopotential height is from the NCEP–NCAR reanalysis (Kalnay et al. 1996), and the daily PNA index is from NOAA CPC.**

positive height anomalies over northwestern North America. In the Pacific sector, the height anomalies represent eastward displacement and meridional focusing of the Asian–Pacific jet (Nigam and Baxter 2015). For monitoring, NOAA's Climate Prediction Center (CPC) calculates the daily PNA index (used here) by projecting daily geopotential height anomalies onto the daily PNA pattern; the latter is computed by interpolating the monthly PNA patterns, which are obtained from a rotated principal component analysis of monthly geopotential height anomalies.

The PNA reigned the Pacific–North American sector in its negative phase from 23 to 29 December 2021, as evidenced by its signature in the upper-level circulation anomalies (Fig. 1a). The four height-anomaly center pattern is a flip of the canonical positive PNA pattern (cf. Fig. 1c). This is especially true for the anomalies centered over northwestern North America: in both the canonical pattern and the Christmas week 2021 pattern, the

anomalies there are largely over land with a somewhat elongated shape in the southwest-to-northeast direction. The intense negative PNA episode during Christmas 2021 evolved from largely positive PNA conditions in November 2021, which transitioned to robust, persistent negative conditions in early December, and peaked around Christmas (Fig. 1f). For comparison, we show another strong negative PNA episode that occurred during 17–23 December 2010 (Fig. 1b), also a La Niña winter. While the height anomaly amplitudes in the two cases are similar, the locations of the anomaly centers exhibit notable differences. In particular, the negative anomalies over northwestern North America in 2010 are largely offshore with a more circular shape; such differences have a bearing on hydroclimate impacts, as noted later.

To put the magnitude of the 2021 Christmas week PNA episode into context, the 7-day mean PNA index during 23–29 December is plotted over a 30-yr period, including December 2021. For this, we first normalized the year-round daily PNA index based on the 1992–2021 climatology, from which 7-day means are computed for 23–29 December of each year. Figure 1d shows the 2021 Christmas week PNA episode to be the strongest 7-day episode in this week (23–29 December) in the last three decades. The 7-day mean value of the PNA index during the 2021 episode fell below minus two standard deviations of the daily PNA index. Extending the comparison to 7-day running means in December across 30 years accords the 2021 Christmas week PNA episode the same rank (Fig. 1e); further analysis (not shown) indicates that it is the strongest 7-day episode in December since 1966. The other negative PNA episode noted above that occurred during 17–23 December 2010 was found to be the second strongest 7-day episode in December during the last three decades (Fig. 1e).

The negative PNA circulation anomalies in Christmas week 2021 are associated with cold near-surface temperature anomalies over the Pacific Northwest (Fig. 2, left), consistent with robust northerly/northwesterly flow along the coast, northeasterlies over British Columbia, and the upslope flow to its east (cf. Fig. 1a and an equivalent-barotropic anomaly structure). Meanwhile, warm anomalies dominate southeastern North America. The dipolar cold–warm anomaly pattern between the northwest and southeast is similar to the climatological PNA surface temperature anomaly pattern shown in Nigam and Baxter (2015). In contrast, the 2010 PNA episode, with its more offshore trough over northwestern North America and thus less exposure to northerly flow (Fig. 1b), is associated with weaker cold anomalies along the coast (Fig. 2, right). The modest differences in circulation and the related but large differences in temperature between the 2021 and 2010 PNA episodes lead to significantly different hydrometeorological impacts, as discussed below.

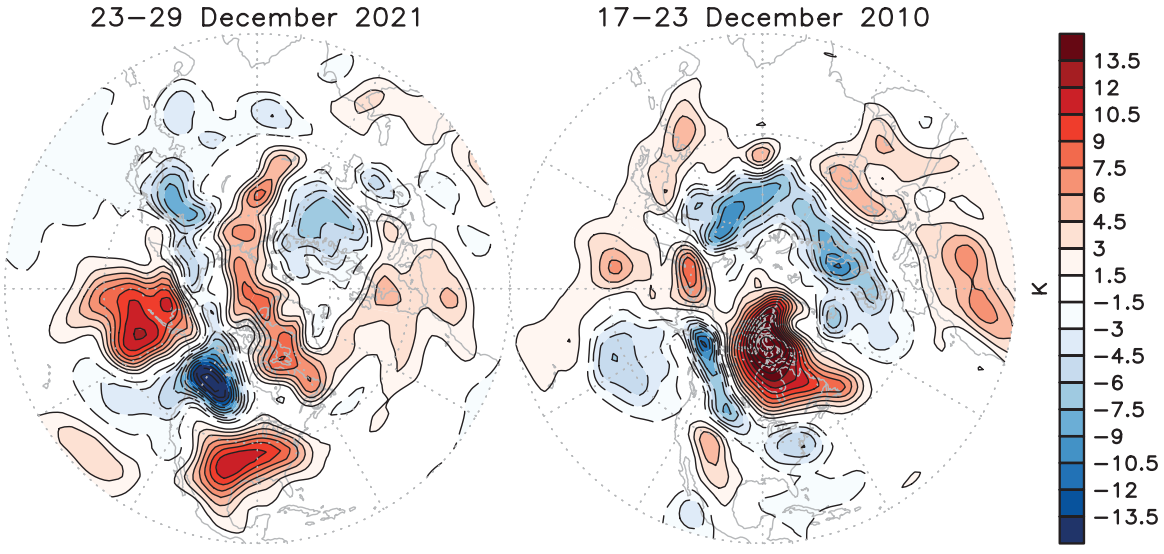


**Fig. 2. Mean 925-hPa temperature anomalies (K) during (left) 23–29 Dec 2021 and (right) 17–23 Dec 2010.**

## Hydrometeorological impacts

The 2021 PNA episode was associated with robust northwesterly onshore flow at upper levels and colder near-surface temperatures, as discussed above. Atmospheric river conditions favored by the negative PNA were present over large stretches of the western United States on 23 December and the southwestern United States on 24 December (not shown). The interaction of these meteorological conditions with the Coastal, Cascade, and Sierra ranges led to blockbuster snowfall and precipitation in the coastal Pacific Northwest. For example, 78 daily snowfall records were broken or tied in Oregon during 23–29 December 2021, primarily to the west of the Cascades (Fig. 3, left), whereas just 4 in the week before and 15 in the week after, both to the east of the Cascades (not shown). In Washington, 20 daily snowfall records were broken or tied during Christmas week, again, primarily to the west of the Cascades; in California, the majority of the 24 broken/tied records were west of the Sierra Nevada (Fig. 3, left). The geographical concentration of snowfall records to the west of the Cascades and Sierra Nevada is consistent with orographic precipitation. While this precipitation is induced by the strong northwesterly onshore (and upslope) flow, its realization as snow stems

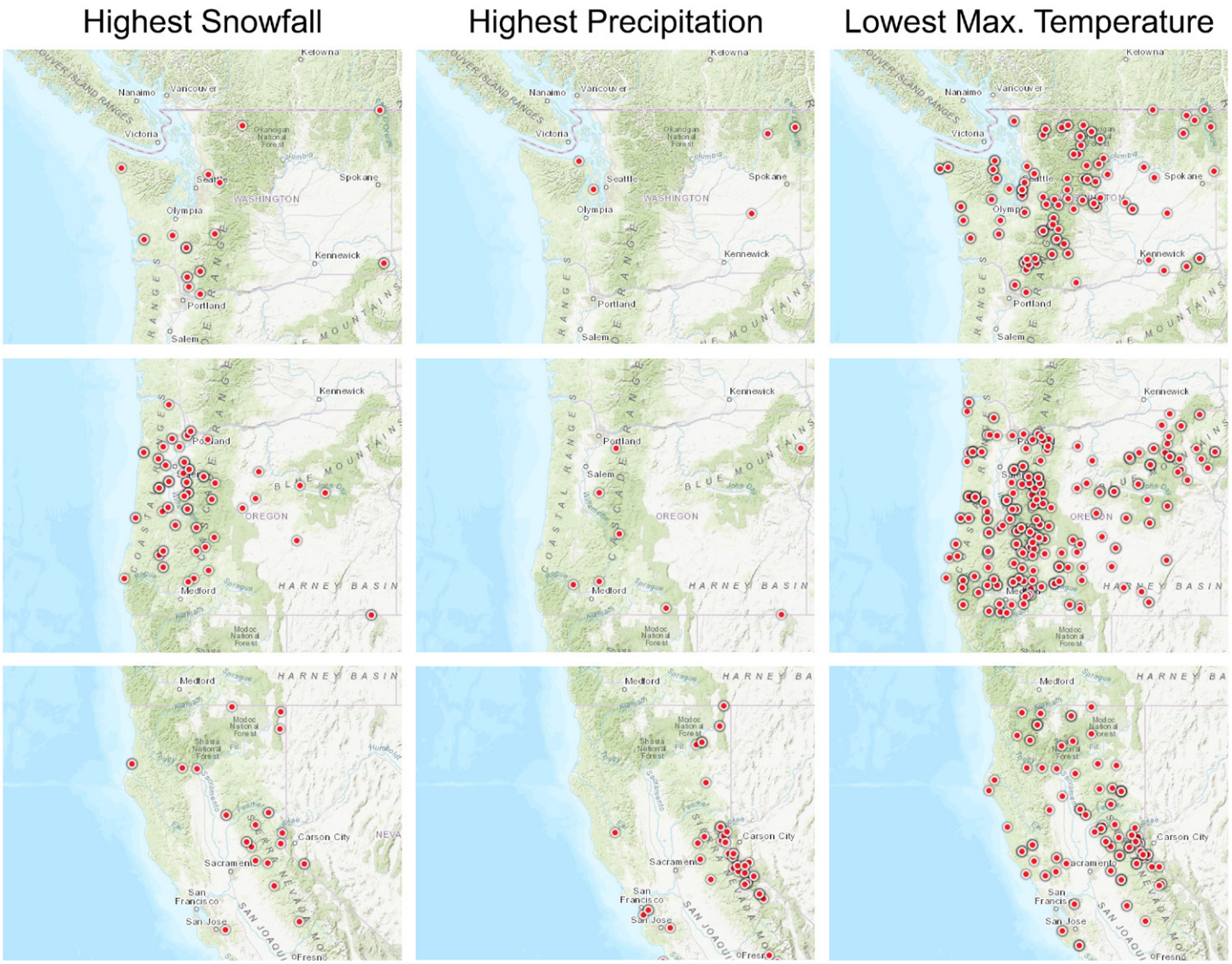


**Fig. 3. Locations of daily records set (ties included) for (left) highest snowfall, (center) highest precipitation, and (right) lowest maximum temperature in (top) Washington, (middle) Oregon, and (bottom) California during the negative PNA episode of 23–29 Dec 2021. Multiple records occurring on different days at the same location are shown as a single dot. Records that occurred in Southern California are not shown but are included in the summary in Table 1. The individual maps were generated interactively using the daily weather records tool at www.ncdc.noaa.gov/cdo-web/datatools/records.**

from the PNA-related cold temperature anomalies in the lower troposphere, especially to the west of the Cascade/Sierra Nevada ranges.

Further examination of total precipitation and temperature records suggests a key role for lower-tropospheric temperature anomalies in generating snowfall records. When measured by total precipitation, only a few records were broken or tied in Washington (6) and Oregon (8) (Fig. 3, center). While a large number of precipitation records were broken or tied in California (105), most were in coastal mountains in Southern California (not shown in Fig. 3), where warmer climatological temperatures preclude snowfall. Precipitation records on the eastern side of the Sierra Nevada did contribute to some snowfall records. The large number of snowfall records in Oregon and Washington without a comparable number of precipitation records can be explained by the record-setting cold temperatures there (Fig. 3, right). We focus on the lowest *maximum* daily temperatures rather than the lowest *minimum* ones because minimum daily temperatures westward of the Cascades are, as it is, near-freezing in December–January. Any additional lowering of minimum temperature from PNA effects (cf. Fig. 2) would thus not be consequential for snowfall; however, snowfall would increase if maximum daily temperatures—around ~40°F in this region—decreased due to PNA effects. The number of daily records set for snowfall, precipitation, and lowest maximum temperature in Washington, Oregon, and California are summarized in Table 1 (upper half).

Compared to the 2021 episode, the 2010 episode set far fewer snowfall records (Table 1, lower half); the ones set were primarily to the east of Cascades (not shown) as opposed to the west in 2021. But many more (in the hundreds) precipitation records were set in 2010 than in 2021, dominated by California as in 2021. The relatively minuscule number of snowfall records, despite the robust number of precipitation records, is entirely consistent with the very small number of temperature records set in 2010 vis-à-vis 2021 (cf. Table 1).

A more spatially complete analysis based on CPC gridded precipitation (Xie et al. 2007) shows the 2021 episode to be associated with wet anomalies stretching nearly the entire coastal western United States, with dry anomalies eastward of the Cascades (Fig. 4, left). The 2010 episode, on the other hand, is associated with dry anomalies over coastal Washington and northern Oregon, weak wet anomalies to the east of Cascades, and strong wet anomalies confined largely to California (Fig. 4, right).

A comparison of the 2010 and 2021 PNA episodes—both with large amplitude and negative phase—shows the hydrometeorological impact of the PNA to be quite sensitive to the precise location of its circulation feature over the Pacific Northwest (onshore versus offshore position) and resulting moisture and temperature advection and orographic interaction. Although different La Niña flavors have similar (and weak) winter hydroclimate footprints over the

**Table 1. Number of daily records set for highest snowfall, highest precipitation, and lowest maximum temperature in Washington, Oregon, and California during the two strong negative PNA episodes of 23–29 Dec 2021 and 17–23 Dec 2010. The two numbers inside the parentheses are the number of records broken and tied, respectively, and the number in front of the parentheses gives the total. The numbers are obtained interactively using the daily weather records tool at www.ncdc.noaa.gov/cdo-web/datatools/records.**

| | Highest snowfall | Highest precipitation | Lowest maximum temperature |
|---|---|---|---|
| | | 2021 episode | |
| Washington | 20 (18 + 2) | 6 (6 + 0) | 152 (138 + 14) |
| Oregon | 78 (71 + 7) | 8 (6 + 2) | 315 (263 + 52) |
| California | 24 (17 + 7) | 105 (94 + 11) | 157 (115 + 42) |
| | | 2010 episode | |
| Washington | 10 (9 + 1) | 4 (3 + 1) | 0 |
| Oregon | 23 (18 + 5) | 39 (31 + 8) | 2 (1 + 1) |
| California | 8 (6 + 2) | 354 (340 + 14) | 6 (1 + 5) |

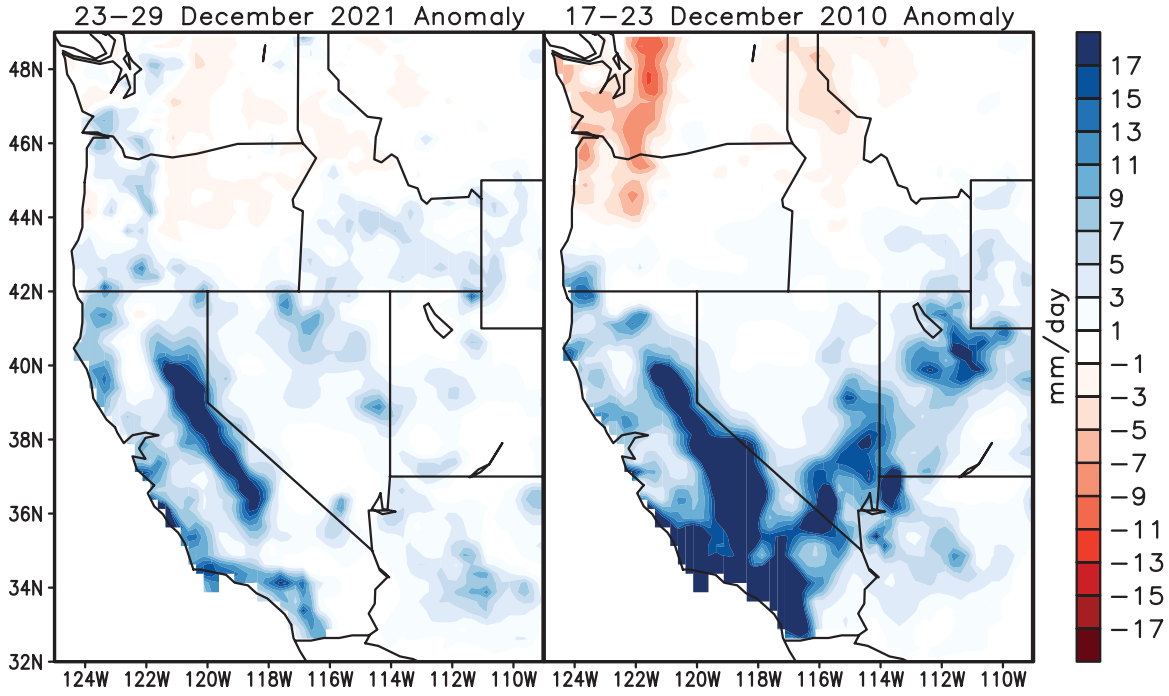


**Fig. 4. Mean precipitation anomalies (mm day$^{-1}$) during (left) 23–29 Dec 2021 and (right) 17–23 Dec 2010. Precipitation data are from CPC Unified Gauge-Based Analysis of Daily Precipitation over CONUS.**

U.S. West Coast, including the Pacific Northwest (cf. Fig. 4 of Wiedermann et al. 2021), they could potentially influence the structure of subseasonal winter variability, including subtle shifts in PNA location.

The tropospheric structure of the temperature anomalies in these two PNA episodes is examined next to better understand the significant influence of related cold temperatures in setting snowfall records.

## Freezing-level height

The atmospheric freezing-level height (FLH) is an often-used diagnostic for cold weather events. The probability of precipitation in the form of snow increases with the lowering of the FLH (Murray 1952), whereas anomalously high FLH could result in rain-on-snow events in snow-covered areas that enhance flood risks (e.g., White et al. 2002; Rössler et al. 2014). In mountainous areas, the FLH relative to elevation provides a useful diagnostic for the snow line.

The mean FLH during 23–29 December 2021 is marked by low values < 750 m over coastal Washington and northern Oregon west of the Cascades (Fig. 5a, shading). The FLH increases southeastward, reaching >2,500 m in Southern California. In Oregon, where most of the snowfall records were set, the FLH is largely between 750 and 1,000 m. The above FLH pattern is a result of strong negative FLH anomalies of <–750 m throughout the coastal western United States (Fig. 5a, contours). The FLH is below the elevation in a relatively coherent band extending from the Cascade to Sierra Nevada ranges, indicating an increased probability of snowfall along the band (Fig. 5b). In contrast, the lowest values of FLH during 17–23 December 2010 are located farther inland and east of the Cascades (Fig. 5c, shading). The associated anomaly pattern is also different from the 2021 episode, with the strongest negative anomalies located in the northeastern corner of the displayed domain and weaker negative anomalies along coastal western United States (Fig. 5c, contours). In Oregon, where fewer snow records were set in the 2010 episode despite the larger number of precipitation records compared to 2021 (Table 1), FLH is between 1,000 and 1,500 m with lower values in the northeast half (Fig. 5c, shading), consistent with the eastward locations of snow records

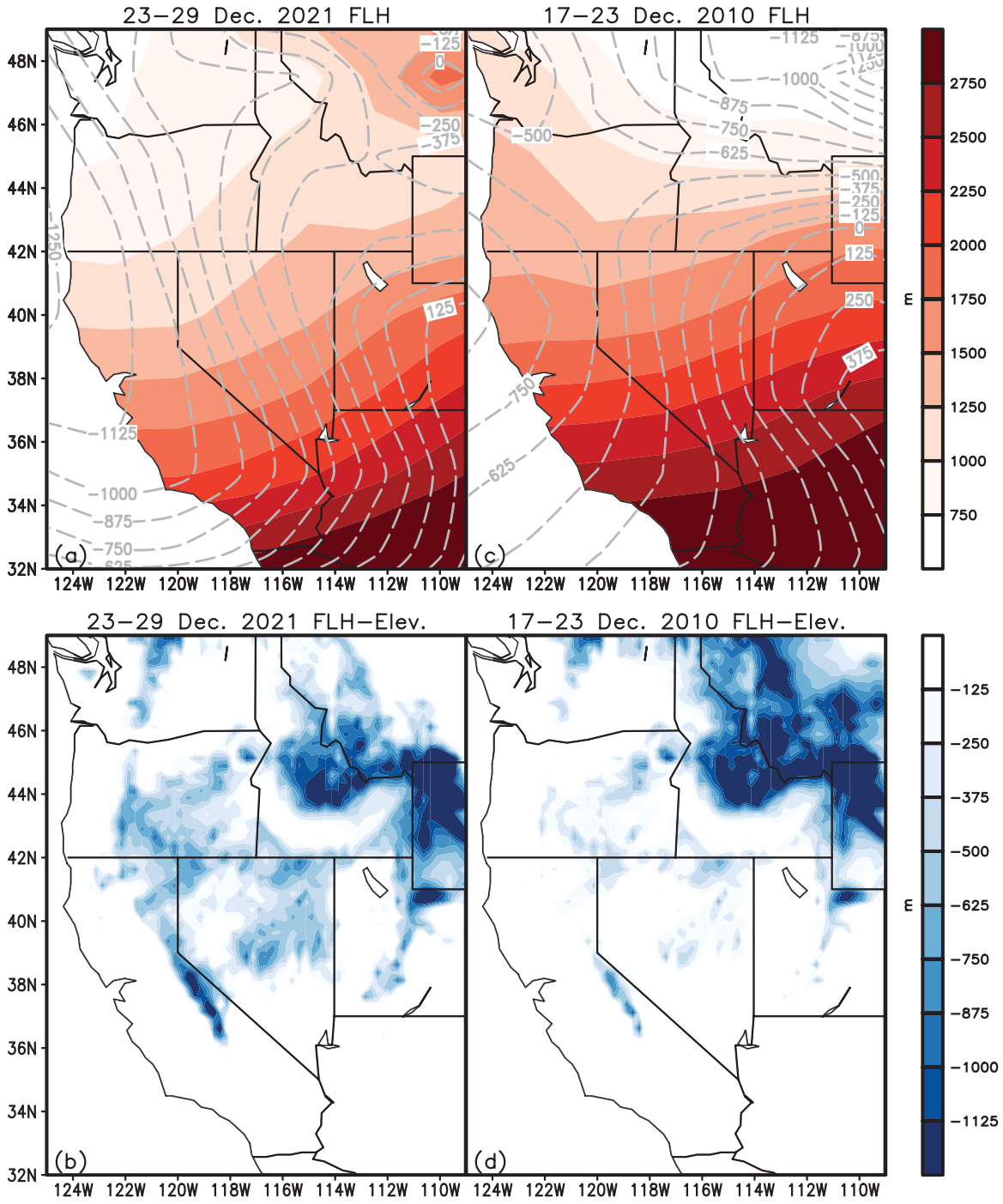


**Fig. 5. (a) Mean FLH (m; shading) and anomalies (m; contours) during 23–29 Dec 2021. (b) FLH minus elevation (m). Positive values are not shaded. (c) As in (a), but for 17–23 Dec 2010. (d) As in (b), but for 17–23 Dec 2010. FLH is derived from the NCEP–NCAR reanalysis based on the hypsometric equation. Elevation data are from GTOPO30 (Danielson and Gesch 2011).**

during this episode. Compared to 2021, the FLH in 2010 is below elevation in scattered and smaller areas, indicating an overall smaller probability of snowfall along the Cascade and Sierra Nevada ranges (Fig. 5d).

## Concluding remarks

Severe weather is of great scientific and societal interest because of related wind/water damage and disruptions, e.g., transportation standstills and power outages. Unraveling the origin of severe weather and whether it is possibly related to climate change is an issue on everyone's mind. In the western United States, advancing subseasonal-to-seasonal prediction

of precipitation is critical for water resource management (Sengupta et al. 2022). By focusing on an eventful week in 2021, we show that La Niña does not have a season-long chokehold on western water resources. PNA-type subseasonal variability can break this chokehold and partially replenish western snowpack and water reservoirs in a week!

It is also seldom that one encounters circulation anomalies consisting of just one winter teleconnection pattern. The Christmas week of 2021 (and its neighboring week in 2010) is thus unique, allowing us to investigate the mechanisms generating the robust and record-setting hydrologic impact of the leading subseasonal teleconnection pattern of northern winter—the Pacific–North American pattern. Our analysis shows how a single, powerful episode of subseasonal variability can recharge water resources in the Pacific Northwest and temporarily dispel the La Niña–induced winter hydrologic gloom. Advancing the understanding of natural variability on subseasonal time scales in the context of seasonal and longer-term climate variability and change can improve water resource management in the drought-plagued western United States.

**Acknowledgments.** BG was supported by the California Department of Water Resources Atmospheric Rivers Program via the University of California, San Diego, and by NASA Grant 80NSSC22K0926.

**Data availability statement.** The following data products are freely available from their web sites: NCEP–NCAR reanalysis (https://psl.noaa.gov/data/gridded/data.ncep.reanalysis.html); CPC Unified Gauge-Based Analysis of Daily Precipitation over CONUS (https://psl.noaa.gov/data/gridded/data.unified.daily.conus.html); daily PNA index (www.cpc.ncep.noaa.gov/products/precip/CWlink/pna/pna.shtml).

## References

Cayan, D. R., 1996: Interannual climate variability and snowpack in the western United States. *J. Climate*, **9**, 928–948, https://doi.org/10.1175/1520-0442(1996)009<0928:ICVASI>2.0.CO;2.

Danielson, J., and D. Gesch, 2011: Global Multi-resolution Terrain Elevation Data 2010 (GMTED2010). USGS Open-File Rep. 2011-1073, 34 pp., https://pubs.usgs.gov/of/2011/1073/pdf/of2011-1073.pdf.

Dettinger, M. D., 2013: Atmospheric rivers as drought busters on the U.S. West Coast. *J. Hydrometeor.*, **14**, 1721–1732, https://doi.org/10.1175/JHM-D-13-02.1.

Ge, Y., and G. Gong, 2009: North American snow depth and climate teleconnection patterns. *J. Climate*, **22**, 217–233, https://doi.org/10.1175/2008JCLI2124.1.

Guan, B., and D. E. Waliser, 2015: Detection of atmospheric rivers: Evaluation and application of an algorithm for global studies. *J. Geophys. Res. Atmos.*, **120**, 12 514–12 535, https://doi.org/10.1002/2015JD024257.

——, N. P. Molotch, D. E. Waliser, E. J. Fetzer, and P. J. Neiman, 2010: Extreme snowfall events linked to atmospheric rivers and surface air temperature via satellite measurements. *Geophys. Res. Lett.*, **37**, L20401, https://doi.org/10.1029/2010GL044696.

——, ——, ——, ——, and ——, 2013: The 2010/2011 snow season in California's Sierra Nevada: Role of atmospheric rivers and modes of large-scale variability. *Water Resour. Res.*, **49**, 6731–6743, https://doi.org/10.1002/wrcr.20537.

Kalnay, E., and Coauthors, 1996: The NCEP/NCAR 40-Year Reanalysis Project. *Bull. Amer. Meteor. Soc.*, **77**, 437–471, https://doi.org/10.1175/1520-0477(1996)077<0437:TNYRP>2.0.CO;2.

Murray, R., 1952: Rain and snow in relation to the 1000–700 mb and 1000-500 mb thicknesses and the freezing level. *Meteor. Mag.*, **81**, 5–8.

Nigam, S., and S. Baxter, 2015: General circulation of the atmosphere | Teleconnections. *Encyclopedia of Atmospheric Sciences*, 2nd ed. Elsevier, 90–109, https://doi.org/10.1016/B978-0-12-382225-3.00400-X.

Ralph, F. M., P. J. Neiman, G. A. Wick, S. I. Gutman, M. D. Dettinger, D. R. Cayan, and A. B. White, 2006: Flooding on California's Russian River: Role of atmospheric rivers. *Geophys. Res. Lett.*, **33**, L13801, https://doi.org/10.1029/2006GL026689.

Rössler, O., P. Froidevaux, U. Börst, R. Rickli, O. Martius, and R. Weingartner, 2014: Retrospective analysis of a nonforecasted rain-on-snow flood in the Alps – A matter of model limitations or unpredictable nature? *Hydrol. Earth Syst. Sci.*, **18**, 2265–2285, https://doi.org/10.5194/hess-18-2265-2014.

Sengupta, A., B. Singh, M. DeFlorio, C. Raymond, A. W. Robertson, X. Zeng, D. E. Waliser, and J. Jones, 2022: Advances in subseasonal to seasonal prediction relevant to water management in the western United States. *Bull. Amer. Meteor. Soc.*, **103**, E2168–E2175, https://doi.org/10.1175/BAMS-D-22-0146.1.

White, A. B., D. J. Gottas, E. T. Strem, F. M. Ralph, and P. J. Neiman, 2002: An automated brightband height detection algorithm for use with Doppler radar spectral moments. *J. Atmos. Oceanic Technol.*, **19**, 687–697, https://doi.org/10.1175/1520-0426(2002)019<0687:AABHDA>2.0.CO;2.

Wiedermann, M., J. F. Siegmund, J. F. Donges, and R. V. Donner, 2021: Differential imprints of distinct ENSO flavors in global patterns of very low and high seasonal precipitation. *Front. Climate*, **3**, 618548, https://doi.org/10.3389/fclim.2021.618548.

Xie, P., M. Chen, S. Yang, A. Yatagai, T. Hayasaka, Y. Fukushima, and C. Liu, 2007: A gauge-based analysis of daily precipitation over East Asia. *J. Hydrometeor.*, **8**, 607–626, https://doi.org/10.1175/JHM583.1.